Measurement of the DAΦNE luminosity with the KLOE detector using large angle Bhabha scattering

The KLOE Collaboration

F. Ambrosino[6], A. Antonelli[2], M. Antonelli[2], C. Bacci[11], P. Beltrame[3], G. Bencivenni[2], S. Bertolucci[2], C. Bini[9], C. Bloise[2], V. Bocci[9], F. Bossi[2], D. Bowring[2,13], P. Branchini[11], R. Caloi[9], P. Campana[2], G. Capon[2], T. Capussela[6], F. Ceradini[11], S. Chi[2], G. Chiefari[6], P. Ciambrone[2], S. Conetti[13], E. De Lucia[2], A. De Santis[9], P. De Simone[2], G. De Zorzi[9], S. Dell'Agnello[2], A. Denig[3,a], A. Di Domenico[9], C. Di Donato[6], S. Di Falco[7], B. Di Micco[11], A. Doria[6], M. Dreucci[2], G. Felici[2], A. Ferrari[2], M.L. Ferrer[2], G. Finocchiaro[2], S. Fiore[9], C. Forti[2], P. Franzini[9], C. Gatti[2], P. Gauzzi[9], S. Giovannella[2], E. Gorini[4], E. Graziani[11], M. Incagli[7], W. Kluge[3], V. Kulikov[5], F. Lacava[9], G. Lanfranchi[2], J. Lee-Franzini[2,12], D. Leone[3], M. Martini[2], P. Massarotti[6], W. Mei[2], S. Meola[6], S. Miscetti[2], M. Moulson[2], S. Müller[2], F. Murtas[2], M. Napolitano[6], F. Nguyen[11,b], M. Palutan[2], E. Pasqualucci[9], A. Passeri[11], V. Patera[2,8], F. Perfetto[6], L. Pontecorvo[9], M. Primavera[4], P. Santangelo[2], E. Santovetti[10], G. Saracino[6], B. Sciascia[2], A. Sciubba[2,8], F. Scuri[7], I. Sfiligoi[2], T. Spadaro[2], M. Testa[9], L. Tortora[11], P. Valente[9], B. Valeriani[3], G. Venanzoni[2], S. Veneziano[9], A. Ventura[4], R. Versaci[2], G. Xu[1,2]

1 Permanent address: Institute of High Energy Physics of Academica Sinica, Beijing, China
2 Laboratori Nazionali di Frascati dell'INFN, Frascati, Italy
3 Institut für Experimentelle Kernphysik, Universität Karlsruhe, Germany
4 Dipartimento di Fisica dell'Università e Sezione INFN, Lecce, Italy
5 Permanent address: Institute for Theoretical and Experimental Physics, Moscow, Russia
6 Dipartimento di Scienze Fisiche dell'Università "Federico II" e Sezione INFN, Napoli, Italy
7 Dipartimento di Fisica dell'Università e Sezione INFN, Pisa, Italy
8 Dipartimento di Energetica dell'Università "La Sapienza", Roma, Italy
9 Dipartimento di Fisica dell'Università "La Sapienza" e Sezione INFN, Roma, Italy
10 Dipartimento di Fisica dell'Università "Tor Vergata" e Sezione INFN, Roma, Italy
11 Dipartimento di Fisica dell'Università "Roma Tre" e Sezione INFN, Roma, Italy
12 Physics Department, State University of New York at Stony Brook, USA
13 Physics Department, University of Virginia, USA

Abstract. We describe the method of measuring the integrated luminosity of the e^+e^- collider DAΦNE, the Frascati ϕ-factory. The measurement is done with the KLOE detector selecting large angle Bhabha scattering events and normalizing them to the effective cross section. The $e^+e^- \to e^+e^-(\gamma)$ cross section is calculated using different event generators which account for the $\mathcal{O}(\alpha)$ radiative initial and final state corrections, and the ϕ resonance contribution. The accuracy of the measurement is 0.6%, where 0.3% comes from systematic errors related to the event counting and 0.5% from theoretical evaluations of the cross section.

1 Introduction

For an accurate measurement of the cross section of an e^+e^- annihilation process, the precise knowledge of the collider luminosity is required. The luminosity depends on three factors: beam-beam crossing frequency, beam currents and the beam overlap area in the crossing region. However, the last quantity is difficult to determine accurately from the collider optics. Thus, experiments prefer to determine the luminosity by the counting rate of well selected events whose cross section is known with good

precision. Since the advent of low luminosity e^+e^- colliders, a great effort was devoted to obtaining good precision in the cross section of electromagnetic processes, extending the pioneer work of the earlier days [1]. At the e^+e^- colliders, working in the range $1\,\text{GeV} < \sqrt{s} < 3\,\text{GeV}$, such as ACO at Orsay, VEPP-II at Novosibirsk, and Adone at Frascati, the luminosity measurement was based on small angle Bhabha scattering, or single and double e^+e^- bremsstrahlung [2,3], thanks to the high statistics. The electromagnetic cross sections scale as $1/s$, while elastic e^+e^- scattering has a steep dependence on the polar angle, $\sim 1/\theta^3$, thus providing high rate for small values of θ. At low and intermediate energy high-luminosity meson factories, the small polar angle region is difficult to access for the

a e-mail: achim.denig@iekp.fzk.de
b e-mail: nguyen@fis.uniroma3.it

presence of the low-beta insertions close to the beam crossing region, while wide angle Bhabha scattering produce a large counting rate and can be exploited for a precise measurement of the luminosity.

We have measured the luminosity counting the number of large angle Bhabha scattering events and normalizing this number to the effective Bhabha cross section σ_{eff}:

$$\int \mathcal{L}\, \mathrm{d}t = \frac{N_{\mathrm{obs}} - N_{\mathrm{bkg}}}{\sigma_{\mathrm{eff}}}\ . \qquad (1)$$

The effective cross section is evaluated by inserting into the detector simulation different event generators which include radiative corrections at a high level of precision. In (1) the number of background events, N_{bkg}, is determined and subtracted from the observed events, N_{obs}.

The main advantages of this method are:

i) high theoretical accuracy by which the cross section could be calculated;

ii) clean event topology of the signal and small amount of background;

iii) large statistics: for $\sigma_{\mathrm{eff}} \sim 430$ nbarn in $45° < \theta_e < 135°$, even at the lowest luminosities obtained in the data taking period, the statistical error $\delta\mathcal{L}/\mathcal{L} \sim 0.3\%$ is reached in about two hours of data taking.

In the following we describe the luminosity measurement using large angle Bhabha scattering. The on-line measurement, with 5% accuracy, was used to provide a fast feedback to DAΦNE. The off-line analysis which is described in this paper reaches a precision of 0.6%, dominated by the uncertainty quoted at present, in the calculation of the Bhabha cross section. A high precision on $\mathcal{L}$ is particularly useful in the KLOE measurement of the hadronic cross section [5].

2 The DAΦNE collider

The DAΦNE e^+e^- collider [4] is designed to run at high luminosity in the energy region corresponding to the resonance $\phi(1020)$. It consists of two independent electron and positron rings of 98 m length with beams that cross at two interaction regions with angle of ~ 25 mrad. DAΦNE was commissioned in 1999 and since 2000 was working with increasing luminosity for three experiments: KLOE, DEAR and FINUDA.

At the end of 2005 KLOE has collected an integrated luminosity of ~ 2.5 fb^{-1}, as shown in Fig. 1. The measurement presented here only refers to the data taken during 2001, although KLOE will use the same luminosity method for the remaining data set.

DAΦNE works in the "topping up" mode, injecting beams with a frequency of about three fillings per hour while the KLOE experiment is continuously taking data. The main beam parameters are presented in Table 1.

In the KLOE interaction region (IR) electron-positron beams cross with a small transverse momentum in the horizontal plane $p_{\mathrm{T}} \sim 13$ MeV/c. The longitudinal and horizontal width of the beam-beam collision region is $\Delta z \sim$
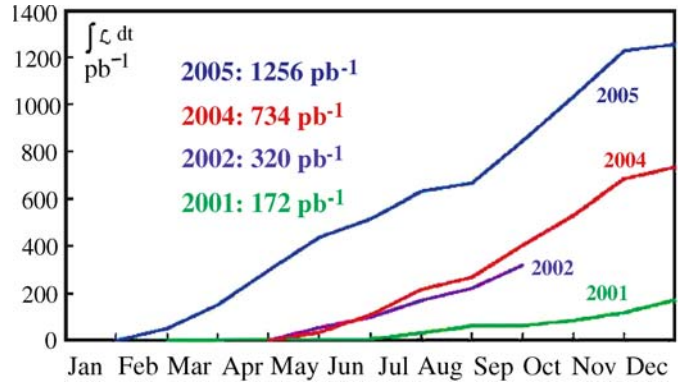

Fig. 1. Luminosity collected by the KLOE experiment from 2001 to 2005

Table 1. Main parameters of the DAΦNE beams during the operation in year 2001

number of bunches (e^+, e^-)	49, 49
current per beam (A)	0.7, 1.0
beam crossing period (ns)	5.43
beam width at crossing:	
σ_x (mm) (horizontal)	2
σ_y (μm) (vertical)	20
σ_z (cm)	3
average luminosity (cm^{-2} s^{-1})	3×10^{31}
luminosity lifetime (min)	30

12 mm and $\Delta x \sim 1.2$ mm respectively. All these quantities are measured run-by-run with very good accuracy ($\sigma_{p_{\mathrm{T}}} \simeq 100$ keV, $\sigma_{\Delta z} \simeq 0.1$ mm, $\sigma_{\Delta x} \simeq 0.05$ mm) detecting large angle Bhabha events as it will be explained in the following. The beam energy spread is (0.302 ± 0.001)MeV, as determined from $\phi \to K_L K_S$ decays.

3 The KLOE detector

A cross view of the detector is shown in Fig. 2. It consists of a large volume drift chamber (DC), a fine grained lead-scintillating fiber sampling calorimeter (EMC) both immersed in a uniform magnetic field of 0.52 T parallel to the beam bisectrix, which is taken as the axis of our coordinate system. The beam pipe around the IR has a spherical shape of 10 cm radius. Three low-beta quadrupoles on either side, at a distance of 50 cm from the IR, fill the space between the beam pipe and the DC inner wall. Two small lead-scintillating tile calorimeters are wrapped around the quadrupoles to complete the EMC hermeticity.

The drift chamber [6], 4 m in diameter and 3.3 m long, is made of 58 concentric rings of drift cells arranged in a full-stereo geometry and is filled with a low Z gas mixture ($90\%\mathrm{He}-10\%i\text{-}\mathrm{C}_4\mathrm{H}_{10}$). Particle trajectories are measured with a space resolution of $\sigma_{xy} \simeq 0.15$ mm and $\sigma_z \simeq 2$ mm; the transverse momentum resolution for long tracks is $\sigma(p_{\mathrm{T}})/p_{\mathrm{T}} \simeq 0.3\%$ and the primary vertex is reconstructed with a space resolution $\simeq 2$ mm. Electrons emitted at large
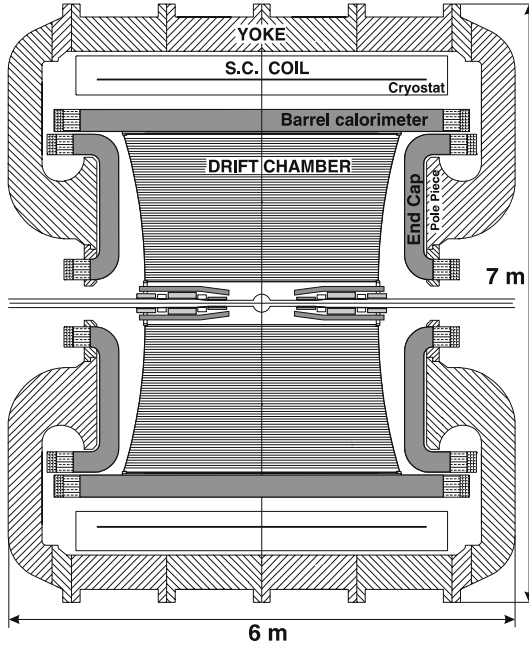
Fig. 2. Cross view of the KLOE detector

angle have a track length greater than 1.5 m and are measured with more than 50 points.

The calorimeter [7] is divided in a barrel ($45° < \theta < 135°$) and two end-caps. It is segmented in depth in five layers, the first four of $\sim 3X_0$ each, and the fifth of $\sim 4X_0$. The barrel is divided in 24 sectors, each sector having 5×12 calorimeter cells of $4 \times 4\,\mathrm{cm}^2$ read out by photomultipliers at both ends to measure the arrival time of particles and to reconstruct the space coordinates. Calorimeter clusters are reconstructed grouping together energy deposits close in space and time. For each cluster, E_{cl} is the sum of the cell energies, the time t_{cl} and position r_{cl} are calculated as energy-weighted averages. The energy, time and position resolutions are $\sigma_{\mathrm{E}}/E = 0.057/\sqrt{E(\mathrm{GeV})}$, $\sigma_t = 54\,\mathrm{ps}/\sqrt{E(\mathrm{GeV})} \oplus 50\,\mathrm{ps}$, $\sigma_{xy} \sim 1.3\,\mathrm{cm}$, and $\sigma_z \sim 1\,\mathrm{cm}/\sqrt{E(\mathrm{GeV})}$.

The trigger [8] is based on the information from the calorimeter and the drift chamber. The EMC trigger requires two distinct energy deposits above threshold ($E > 50\,\mathrm{MeV}$ in the barrel and $E > 150\,\mathrm{MeV}$ in the end-caps). The DC trigger is based on the number of drift cells that recorded a hit and on their topology. Recognition and rejection of cosmic ray events is also done at trigger level: events with two energy deposits above 30 MeV in the fifth calorimeter layer are vetoed. The trigger is synchronized with the DAΦNE RF divided by 4, $T_{\mathrm{sync}} = 10.86\,\mathrm{ns}$, with an accuracy of 50 ps. The time of the bunch crossing producing an event is determined after event reconstruction.

4 The selection of Bhabha scattering events

An on-line filter selects Large Angle Bhabha (`LAB`) events using only calorimeter information, to minimize the CPU

time necessary for the whole event reconstruction; while a more refined off-line analysis is done selecting Very Large Angle Bhabha (`VLAB`) events, tightening the acceptance cuts and including also the tracking information.

The `LAB` selection is based on the calorimeter clusters energy, position and timing; the angle of a cluster is defined by its coordinates, r_{cl}, and the average position of the interaction point. We require:

1) at least two calorimeter clusters with energy $300\,\mathrm{MeV} < E_{\mathrm{cl}} < 800\,\mathrm{MeV}$ and polar angle $45° < \theta_{\mathrm{cl}} < 135°$;
2) among all cluster pairs, the two clusters with the minimum polar angle acollinearity, $\zeta = |\theta_{\mathrm{cl}1} + \theta_{\mathrm{cl}2} - 180°|$, are selected and ζ is required to be smaller than $10°$;
3) the two selected clusters should satisfy the timing condition $|t_{\mathrm{cl}1} - t_{\mathrm{cl}2}| < 4\,\mathrm{ns}$.

The selected sample contains also $e^+e^- \to \gamma\gamma$ events, which are collinear in the transverse plane. To eliminate these events we further require:

4) the angle in space between the two clusters must satisfy $\cos \alpha > -0.975$, where $\cos \alpha = r_{\mathrm{cl}1} \cdot r_{\mathrm{cl}2}/|r_{\mathrm{cl}1}|\,|r_{\mathrm{cl}2}|$;
5) the presence of at least 50 DC hits in the event.

The precision with which `LAB` events are selected is about 1% and is limited by the energy resolution of the calorimeter ($\sigma_{\mathrm{E}} \simeq 40\,\mathrm{MeV}$ for $E_{\mathrm{cl}} = 510\,\mathrm{MeV}$). By adding information from the tracking chamber, the precision is considerably improved and the background of $\pi^+\pi^-$ and $\mu^+\mu^-$ events (1.2% contamination at this level) is further reduced.

In the `VLAB` selection the tracking information gives the momentum measurement and the charge assignment, while the information on polar angles is still taken from the EMC clusters. There is no need to use the tracks for the angular information since calorimeter clusters and tracks have similar angular resolutions ($\sigma_\theta \simeq 1°$) and hence no further systematic uncertainty is introduced. The selection cuts of `VLAB` events are slightly tighter than in the `LAB` selection; the event must satisfy the following requirements:

1) for the two tracks with the largest number of associated hits, the point-of-closest-approach to the origin (PCA) must be within $(x_{\mathrm{pca}}^2 + y_{\mathrm{pca}}^2)^{1/2} < 7.5\,\mathrm{cm}$ and $|z_{\mathrm{pca}}| < 15\,\mathrm{cm}$;
2) the two tracks must have opposite curvature;
3) both tracks must have momentum $p \geq 400\,\mathrm{MeV}$;
4) the two EMC clusters selected by the `LAB` filter must have polar angle $55° < \theta_{\mathrm{cl}} < 125°$;
5) the cut on the polar angle acollinearity for the two `LAB` clusters is further tightened to $\zeta < 9°$.

5 Evaluation of efficiencies

The effective `VLAB` cross section is obtained from Monte Carlo, it is therefore important to check that the resolution of the variables and the efficiency of the selection are well reproduced by the detector simulation, and to correct for any mismatch between data and Monte Carlo. In particular a difference in the resolution of the kinematic variables
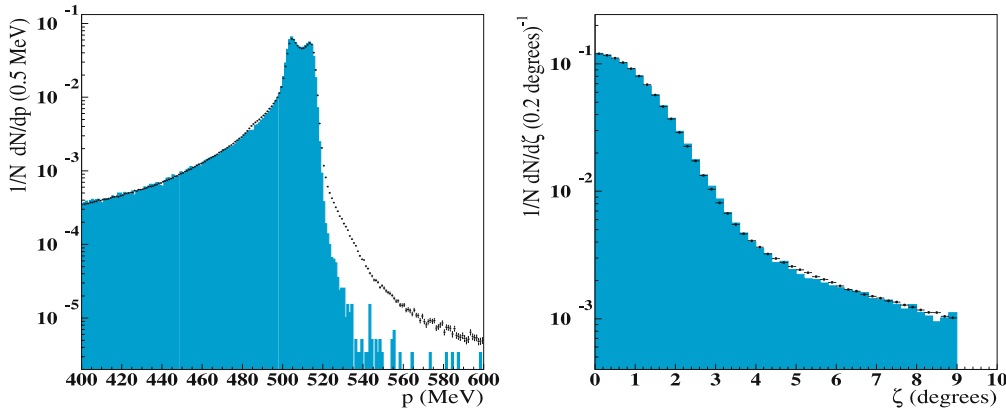
Fig. 3. Comparison between data (*points*) and Monte Carlo (*histogram*) distributions for the track momentum p (*left*) and for the energy clusters acollinearity ζ (*right*)

can give rise to systematic effects at the borders of the chosen phase space. The studies presented here refer to the data sample collected in 2001 because these data have been used for the measurement of the pion form factor [5]. Since 2002 the cosmic ray veto has been improved and a smaller systematic error from this effect should be accounted for in later data.

5.1 Angular acceptance

Figure 3 shows the comparison of data with the Monte Carlo simulation[1] for the distributions of momentum, p, and acollinearity, ζ. In both variables, the cuts $p > 400$ MeV and $\zeta < 9°$ occur where the agreement is very good. Furthermore, both variables are cut in a region where eventual resolution mismatches between data and Monte Carlo have small effects, because far from the bulk of the distribution. Thus, any systematic error from the cuts on p and ζ is considered as negligible. The difference observed at high particle momenta is due to non-Gaussian tails in the DC reconstruction which are not simulated in Monte Carlo. However, since no high-momentum cut is applied in the selection, no systematic effect arises from this small difference.

The situation is different for the requirement on the polar angle, θ. In this case the cut $55° < \theta < 125°$ is applied in a region with a steep rise of the distribution, with a priori possible large systematic effects. Figure 4 shows the comparison of the data and the simulated distribution, both normalized to the total number of events: the overall agreement is very good. The polar angle resolution from the measurement of the calorimeter clusters is $\sim 1°$, therefore a net gain or loss of events due to a systematic difference between the polar angle resolution in data and Monte Carlo can only occur in the bins close to the borders. To evaluate the effect, the relative difference between data and Monte Carlo is computed in the border intervals ($55° < \theta < 65°$, $115° < \theta < 125°$), after normalizing the number of Monte Carlo events, N_{MC}, to coincide with the number of
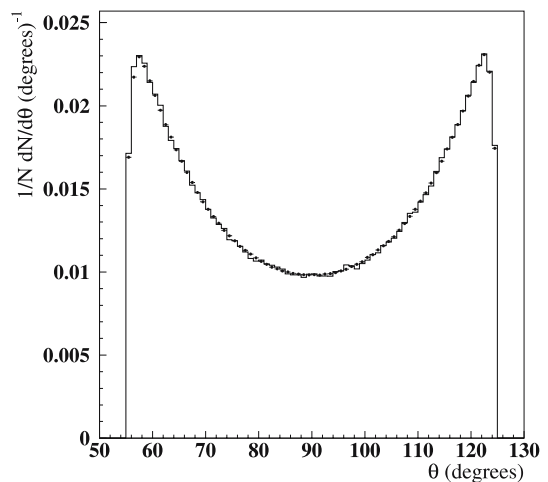

Fig. 4. Comparison between the data (*points*) and Monte Carlo (*histogram*) distributions of energy clusters polar angle normalized to the same number of events

data events, N_{data}, in the central region ($65° < \theta < 115°$): the value $(N_{\mathrm{data}} - N_{\mathrm{MC}})/N_{\mathrm{data}} = (-0.25 \pm 0.03)\%$ is used both as the relative correction to the effective cross section and as systematic uncertainty on the angular acceptance. This estimate is confirmed by computing the relative variation of the luminosity as a function of the value of the cut in polar angle, θ_{cut}:

$$\frac{\Delta\mathcal{L}}{\mathcal{L}} = \frac{N_{\mathrm{VLAB}}(\theta_{\mathrm{cut}} < \theta < 180° - \theta_{\mathrm{cut}})}{N_{\mathrm{VLAB}}(55° < \theta < 125°)}$$
$$- \frac{\sigma_{\mathrm{eff}}(\theta_{\mathrm{cut}} < \theta < 180° - \theta_{\mathrm{cut}})}{\sigma_{\mathrm{eff}}(55° < \theta < 125°)} .$$

The behaviour of $\Delta\mathcal{L}/\mathcal{L}$ as a function of θ_{cut} shows that, in a 5° range, the relative variation is $\Delta\mathcal{L}/\mathcal{L} = {}^{+0.003}_{-0.002}$, consistent with the quoted systematic error.

5.2 Tracking efficiency

To evaluate the tracking efficiency we use LAB events because no tracking information is required in selecting this

---

[1] Hereafter we will implicitly refer to the event generator Babayaga, Version 3.5. This and other generators will be discussed in Sect. 7.

sample. Thus, we select events with a tagging track having $p_{\text{tag}} > 400\,\text{MeV}$ and associated to one of the two `LAB` clusters.

In this subsample, we define the tracking efficiency ϵ_{track} as the fraction of events which fulfil the following requirements:

1) at least a second track associated to the origin (as defined above), this track must be one of the two with the largest number of associated hits;
2) the track must have momentum $p_2 > 400\,\text{MeV}$ and curvature opposite to the tagging track;
3) the distance d between the first hits of tagging and candidate track must be larger than 50 cm.

We have verified that varying the values for d, p_{tag}, p_2 the tracking efficiency ϵ_{track} is stable and we find that the efficiency for data and Monte Carlo are:

$$\epsilon_{\text{track}}^{\text{data}} = (99.824 \pm 0.005)\%$$
$$\epsilon_{\text{track}}^{\text{MC}} = (99.764 \pm 0.011)\%\,,$$

where the errors are statistical. The relative difference $\Delta\epsilon_{\text{track}} = (6.0 \pm 1.2) \times 10^{-4}$ is taken as the systematic uncertainty due to the tracking efficiency.

5.3 Cluster efficiency

To evaluate the cluster efficiency we select a subsample based on the tracking information. Wa ask for two and only two tracks with the following requirements:

– the two tracks are connected to one and only one vertex located at $|r| < 5\,\text{cm}$;
– both tracks are emitted at polar angle $50° < \theta < 130°$, where θ is measured at the vertex position;
– both tracks fulfil the same requirements on the radial position of their first hit (fh) and last hit (lh) in the DC: $(x_{\text{fh}}^2 + y_{\text{fh}}^2)^{1/2} < 40\,\text{cm}$ and $(x_{\text{lh}}^2 + y_{\text{lh}}^2)^{1/2} > 180\,\text{cm}$ (these requirements exclude splitted tracks);
– the electron–positron invariant mass, $M_{\text{e e}}$, must be in the range $1017.5\,\text{MeV/c}^2 < M_{\text{e e}} < 1021.5\,\text{MeV/c}^2$;
– the track mass, m_{trk}, defined as the mass associated to the momenta p_1 and p_2 under the hypothesis of a final state of two charged particles of the same mass and one photon, should be smaller than 90 MeV,

$$\sqrt{|p_1|^2 + m_{\text{trk}}^2} + \sqrt{|p_2|^2 + m_{\text{trk}}^2} + |p_1 + p_2 - p_b| = \sqrt{s}$$

here p_b is the average beam-beam transverse momentum measured run by run.

The last two cuts efficiently remove the background from $\mu^+\mu^-$ and $\pi^+\pi^-$ events. We then look for two calorimeter clusters satisfying the requirements:

1) $|\rho_{\text{lh}} - \rho_{\text{cl}}| < \Delta\rho = 40\,\text{cm}$, ρ_{cl} being the position of the cluster in the x-y plane; this defines the cluster to track association;
2) $|p - E_{\text{cl}}| < \Delta E = 210\,\text{MeV}$;
3) $|t_{\text{cl}1} - t_{\text{cl}2}| < \Delta t = 4\,\text{ns}$.

The cluster efficiency $\epsilon_{\text{cluster}}$ is defined as the fraction of events in the control sample which fulfil the requirements.

We have verified that varying the values for $\Delta\rho$, Δt and ΔE the efficiency is stable and we find that the values for data and Monte Carlo are in good agreement:

$$\epsilon_{\text{cluster}}^{\text{data}} = (99.58 \pm 0.11)\%$$
$$\epsilon_{\text{cluster}}^{\text{MC}} = (99.65 \pm 0.02)\%\,,$$

where the errors are statistical.

To evaluate the systematic uncertainty, the inefficiency in data has been studied and understood as due to cluster splitting, in which a cluster is split into two clusters neither of them surviving the lower energy cut. A correction of $\delta_{\text{split}} = (0.135 \pm 0.007)\%$ is applied to $\epsilon_{\text{cluster}}^{\text{MC}}$, and the following difference between data and Monte Carlo is obtained:

$$\Delta\epsilon_{\text{cluster}} = \epsilon_{\text{cluster}}^{\text{data}} - \epsilon_{\text{cluster}}^{\text{MC}} = (0.07 \pm 0.11)\%\,.$$

Since both data and Monte Carlo agree within statistical errors, we take the value 0.11% as the systematic uncertainty in the cluster efficiency.

5.4 Background

Given the cut on the track momentum, $p > 400\,\text{MeV}$, the only relevant background processes are $e^+e^- \to \mu^+\mu^-$ and $e^+e^- \to \pi^+\pi^-$. The estimate of this background is based on the track mass variable, m_{trk}. Figure 5 shows the m_{trk} distribution for a sample of `VLAB` events: besides Bhabha scattering events, clustered at low values of m_{trk}, the only significant structure is the peak associated with $\pi^+\pi^-$ events around $m_{\text{trk}} \simeq 136\,\text{MeV}$. There is no evidence for background from $\mu^+\mu^-$ events because of the lower cross section and of the smaller efficiency to release clusters with $E > 300\,\text{MeV}$. We have used two methods to measure the amount of background: the first consists in fitting the track mass distribution, while in the second method we use particle identification based on time of flight method for discriminating pions (muons) from electrons, called `PID` function in the following.

1. The `PID` function exploits the time of flight and the different shape of energy deposits in the calorimeter
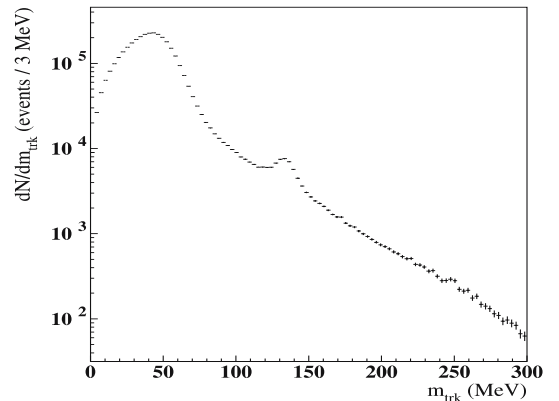

Fig. 5. m_{trk} distribution for a sample of `VLAB` events

layers, of clusters associated to tracks to discriminate pions (muons) from electrons on an event-by-event basis [5]. The fraction of background is evaluated from events in which at least one track has been identified by the PID function as a pion,

$$\frac{N_{\mathrm{bkg}}}{N_{\mathrm{VLAB}}} = (0.623 \pm 0.015)\%$$

2. The m_{trk} distribution from Monte Carlo is well described by an exponential function in the range 100 MeV $< m_{\mathrm{trk}} < 170$ MeV. We fit the m_{trk} distribution in this range with a Gaussian (background) plus an exponential function (signal): the relative amount of background is

$$\frac{N_{\mathrm{bkg}}}{N_{\mathrm{VLAB}}} = (0.54 \pm 0.13)\%,$$

Since the previous results are in agreement within statistical errors, we take the value 0.13% as the systematic uncertainty and $N_{\mathrm{bkg}}/N_{\mathrm{VLAB}} = 0.62\%$ as the background contamination in VLAB event sample.

5.5 Cosmic veto

Cosmic ray events are vetoed at the trigger level, but a fraction of these events is flagged and recorded for calibration with a downscale factor of 5. Applying the VLAB selection on the downscaled events, we estimate the total fraction of VLAB events lost due the trigger veto directly from data. The effect is stable in time and an average correction of $(0.40 \pm 0.03)\%$ has been applied to the effective cross section evaluated with Monte Carlo.

6 Evaluation of systematic effects

The effects on the acceptance and efficiency discussed so far do not show variations in time and therefore average corrections were applied to the whole data set. Other effects depend on the actual run conditions and there was need to determine the corrections on a run-by-run basis. As will be shown, these time dependent effects are very small. In particular they are related to energy calibration and to variations in the center of mass energy.

6.1 Calorimeter energy calibration

We have studied the effect of a variation of the calorimeter energy scale on the LAB selection, which requires two energy clusters in the interval 300–800 MeV and we have computed the effect of these variations on the VLAB selection. The 2001 data sample consists of three periods, where the EMC energy scale changed by 1%, for an energy resolution of 8%. For each period, the E_{cl} distribution is evaluated and compared with the Monte Carlo distribution (see Fig. 6). We observe that i) the Monte Carlo overestimates the high energy tail of the distribution, and ii) there are systematic shifts in the E_{cl} mean value.
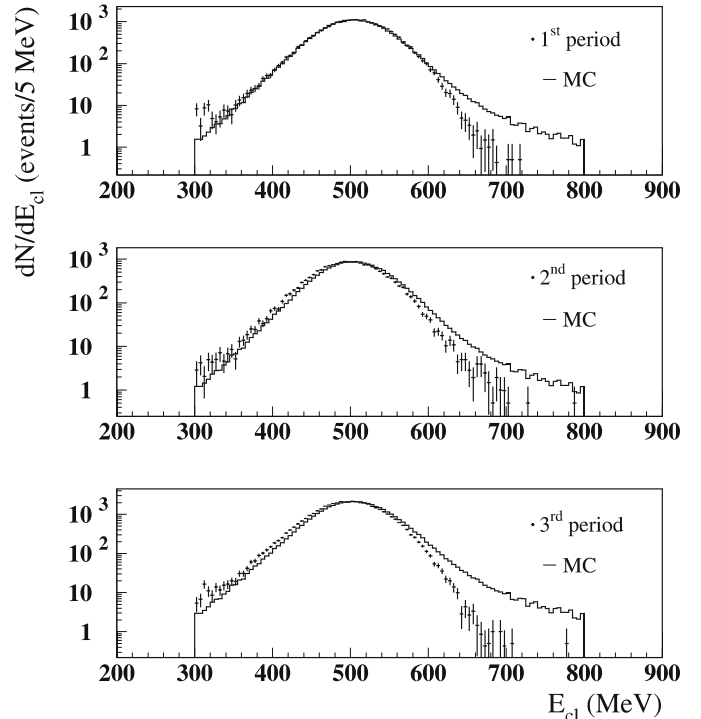

Fig. 6. Distribution of the cluster energy of VLAB events for three runs (*points*), one from each of the three different periods of data taking, compared with Monte Carlo (*solid line*)

We have calculated the systematic effect due to overestimating the high energy tail by extrapolating the Monte Carlo distribution above 800 MeV. The relative difference between data and Monte Carlo amounts to $\Delta_{E_{\mathrm{tail}}} = (6.1 \pm 1.6) \times 10^{-4}$. The value $\Delta_{E_{\mathrm{tail}}}$ is taken as the systematic uncertainty due to different high energy tails between data and Monte Carlo.

The effect of the shift of the energy distribution between data and Monte Carlo has been estimated by taking the difference between the mean values of the distributions as a measurement of the shift and by adding (subtracting) the events, which are gained (lost) according to this shift. The run-by-run weighted average is $\Delta_{E_{\mathrm{calib}}} = (6 \pm 2) \times 10^{-4}$, and it has been considered as the relative systematic error due to variations in the calorimeter energy calibration. Furthermore we have checked that, aside from a coherent shift, the shape of the cluster energy distribution in VLAB events is the same in the three periods (see Fig. 6).

The overall systematic error due to the calorimeter energy calibration is

$$\Delta_{E_{\mathrm{cl}}} = \Delta_{E_{\mathrm{tail}}} \oplus \Delta_{E_{\mathrm{calib}}} = 8.6 \times 10^{-4}.$$

Since the two effects tend to compensate, no correction was applied to the luminosity measurement.

6.2 Center of mass energy

The effective VLAB cross section is evaluated by Monte Carlo at the average value of the center of mass energy,
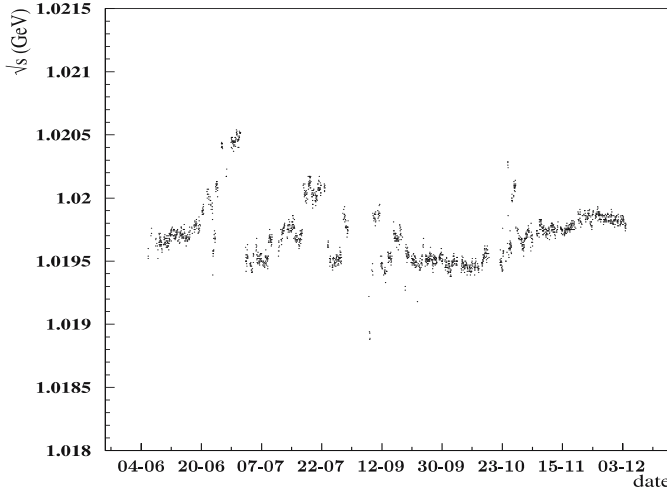
Fig. 7. Distribution of the center of mass energy as a function of time in 2001

Fig. 8. Top: comparison between Babayaga (*histogram*) and Bhwide (*points*) for the differential cross section as function of the acollinearity (after momentum and polar angle cuts). **Bottom**: comparison between Babayaga and Bhwide for the differential cross section as function of the missing energy fraction, $v = 1 - M^2/s$ (after momentum, polar angle and acollinearity cuts)

$\sqrt{s} = 1.0195$ GeV. To account for variations of the beam energy, we corrected the luminosity measurement for the relative change in cross section, $\Delta\mathcal{L}/\mathcal{L}_0 = -\Delta\sigma/\sigma_0$, where $\mathcal{L}_0$ is the luminosity obtained with the nominal cross section $\sigma_0 = \sigma_{\text{eff}}(1.0195$ GeV$)$. The VLAB events energy scale was calibrated with the well measured value of M_ϕ [18] during an energy scan [19] around the ϕ resonance. Figure 7 shows as a function of time the value of $\sqrt{s}$ measured from VLAB events: variations in $\sqrt{s}$ never exceed a few hundred keV, and single run corrections are always smaller than 0.5%. The average correction is 0.1% and we consider this value also as the systematic uncertainty for this effect.

7 The VLAB cross section

The event generators Babayaga [9,10] and Bhagenf [11], developed for the large angle Bhabha scattering at DAΦNE and based on the cross section calculated in [12], have been interfaced with the detector simulation program GEANFI [13] for evaluating the effective cross section, as well as for estimating the systematic uncertainties. After applying the VLAB selection we find an agreement better than 0.1% between the cross sections calculated with the two generators, including the event reconstruction efficiency:

$$\text{Babayaga} \quad \sigma_{\text{eff}} = (431.0 \pm 0.3)\text{nb}$$
$$\text{Bhagenf} \quad \sigma_{\text{eff}} = (430.7 \pm 0.3)\text{nb}.$$

The error given in the above cross section is due to the Monte Carlo statistics. The systematic theoretical uncertainty claimed by the authors is 0.5% in both cases. The radiative corrections due to the treatment of initial and final state radiation in Bhagenf and Babayaga have been compared with two other event generators: the Bhwide code [14] developed for LEP and the Mcgpj code [15] developed for VEPP-2M and based on the cross section calculated in [16]. Further details on the event generators
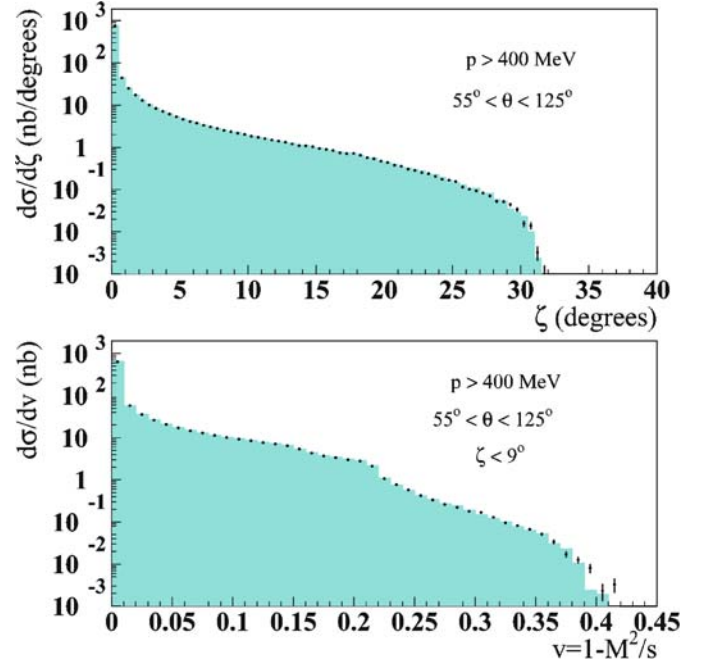
and the application in the analysis can be found in reference [17]. For this comparison, we applied the kinematic VLAB requirements on the generated momenta and computed the VLAB cross sections for the four generators, as shown in the table below, where errors are due to Monte Carlo statistics.

MC code	σ (nb)
Bhagenf	460.8 ± 0.1
Babayaga	459.4 ± 0.1
Mcgpj	457.4 ± 0.1
Bhwide	456.2 ± 0.1

These values are obtained without considering detector smearing and loss effects and therefore the results are considerably different from the effective VLAB cross section presented before, where a full detector simulation was performed. Moreover, contributions from the ϕ decay and vacuum polarization effects are not applied, because they are the same for all generators.

The agreement among the four generators supports the systematic uncertainty of 0.5% quoted by the authors of Bhagenf and Babayaga.

Moreover, we have compared the differential distributions for the acollinearity ζ and the missing energy fraction $v = 1 - M_{\text{ee}}^2/s$, which are very sensitive to the difference in the treatment of radiative effects. Also in this case we find good agreement as can be seen in Fig. 8.

8 Results

The analysis refers to the data taken during the year 2001 for an integrated luminosity of $141\,\mathrm{pb}^{-1}$. All corrections and systematic errors discussed above are summarized in Table 2. Summing all errors in quadrature, the relative experimental uncertainty for the luminosity measurement using Bhabha scattering events is $\delta\mathcal{L}_{\mathrm{exp}}/\mathcal{L}_{\mathrm{exp}} = 0.3\%$.

Different event generators were used to evaluate the cross section, the comparison shows good agreement in the distributions of the variables used to select the events and in the value of σ_{eff}. The value of the effective `VLAB` cross section has been calculated with the `Babayaga` event generator that has been interfaced with the `GEANFI` simulation program. We use a theoretical uncertainty of 0.5%, that is quoted by the authors of `Bhagenf` and `Babayaga` (an improvement by more than a factor 2 is currently in progress [20]) and it is confirmed by the comparison with other event generators.

The total error of the luminosity measurement is then

$$\frac{\delta\mathcal{L}}{\mathcal{L}} = \frac{\delta\mathcal{L}_{\mathrm{exp}}}{\mathcal{L}_{\mathrm{exp}}} \oplus \frac{\delta\sigma_{\mathrm{eff}}}{\sigma_{\mathrm{eff}}} = 0.6\%\,.$$

Table 2. Summary of the corrections and systematic errors in the measurement of the luminosity

	correction (%)	systematic error (%)
angular acceptance	+0.25	0.25
tracking	–	0.06
clustering	+0.14	0.11
background	−0.62	0.13
cosmic veto	+0.40	–
energy calibration	–	0.10
center of mass energy	+0.10	0.10
	+0.34	0.32

References

1. N. Cabibbo, R. Gatto, Phys.Rev. **125**, 1577 (1961)
2. G. Barbiellini et al., Nucl. Instrum. Method **123**, 125 (1975)
3. H.C. Dehne et al., Nucl. Instrum. Method **116**, 345 (1974)
4. C. Guiducci et al., "DAΦNE", presented at the Workshop on e^+e^- Colliders in the 1–2 GeV Range, Alghero, Italy, September 2003, e-Print Archive: physics/0403014
5. KLOE Collaboration, A. Aloisio et al., Phys. Lett. B **606**, 12 (2005)
6. KLOE Collaboration, M. Adinolfi et al., Nucl. Instrum. Method A **488**, 51 (2002)
7. KLOE Collaboration, M. Adinolfi et al., Nucl. Instrum. Method A **482**, 364 (2002)
8. KLOE Collaboration, M. Adinolfi et al., Nucl. Instrum. Method A **492**, 134 (2002)
9. C.M. Carloni Calame et al., Nucl. Phys. B **584**, 459 (2000)
10. C.M. Carloni Calame, Phys. Lett. B **520**, 16 (2001)
11. E. Drago, G. Venanzoni, "A Bhabha generator for DAΦNE including radiative corrections and Φ resonance", report INFN-AE-97-48
12. F.A. Berends, R. Kleiss, Nucl. Phys. B **228**, 537 (1983)
13. KLOE Collaboration, F. Ambrosino et al., Nucl. Instrum. Method A **534**, 403 (2004)
14. S. Jadach, W. Placzek, B.F.L. Ward, Phys. Lett. B **390**, 298 (1997)
15. G.V. Fedotovich, A.L. Sibidanov, Nucl. Phys. B (Proc. Suppl.) **131**, 9 (2004)
16. A.B. Arbuzov et al., JHEP **9710**, 001 (1997)
17. A. Denig, F. Nguyen, "The KLOE luminosity measurement", KLOE note n.202, July 2005, www.lnf.infn.it/kloe/pub/knote/kn202.ps
18. CMD–2 Collaboration, R.R. Akhmetshin et al., Phys. Lett. B **578**, 285 (2004)
19. KLOE Collaboration, F. Ambrosino et al., Phys. Lett. B **608**, 199 (2005)
20. C.M.C. Calame, "Babayaga at NLO", presented at the Workshop, "e^+e^- Collisions from ϕ to ψ", Novosibirsk, Russia, February 2006, www.inp.nsk.su/conf/phipsi06/